IEEE Access
Multidisciplinary ⋮ Rapid Review ⋮ Open Access Journal

Received May 31, 2021, accepted June 10, 2021, date of publication June 16, 2021, date of current version June 28, 2021.

Digital Object Identifier 10.1109/ACCESS.2021.3089820

Mining Subsidence Prediction Parameter Inversion by Combining GNSS and DInSAR Deformation Measurements

GUORUI WANG[1,2,3], QIANG WU[1,3], PEIXIAN LI[1], XIMIN CUI[1], YONGFENG GONG[2], JIA ZHANG[2], AND WEI TANG[1]

[1]College of Geoscience and Surveying Engineering, China University of Mining and Technology (Beijing), Beijing 100083, China
[2]Institute of Land and Resources Investigation and Monitoring, Ningxia Hui Autonomous Region, Yinchuan 750000, China
[3]National Coal Mine Water Hazard Prevention Engineering Technology Research Center, Beijing 100083, China

Corresponding author: Peixian Li (pxlicumt@126.com)

This work was supported in part by the funds from the Natural Science Foundation of Ningxia Hui Autonomous Region under Grant 2020AAC03476 and Grant 2020AAC03477, and in part by the Fundamental Research Funds for the Central Universities under Grant 2020YQDC05 and Grant 2021YQDC01.

ABSTRACT Line of Sight (LOS) deformation based on Differential Interferometric Synthetic Aperture Radar (DInSAR) techniques cannot be used in traditional probability integration method (PIM) parameter inversion. To improve the accuracy of parameter inversion, a model based on 3D deformation was proposed. The model simulates 3D deformation using PIM directly. The inverse of the Sum of the Squared Errors (SSE) of the PIM results and the measured deformation results was used as a fitting function within the GA. Reliable PIM parameters can be obtained based on this GA model. To identify the surface movement law of the Jinfeng coal mine, 6 Global Navigation Satellite System (GNSS) monitor points were established over the 011207 and 011809 working panels. Due to the limited number of points and the large distance between the points, it is not sufficient to obtain reliable PIM parameters using GNSS only. As a complement, 83 Sentinel-1A images were analyzed with small baseline subset (SBAS) DInSAR, and the LOS direction deformation was obtained. The reliable PIM parameters were calculated with the 3D inversion model based on the combination of LOS direction deformation and GNSS-monitored deformation. Then, those parameters were used to predict the coal mine deformation of panels 011207 and 011809, which demonstrated that the prediction results coincide with the measured results. The model can be used to study the laws of mining subsidence combined with DInSAR and GNSS, which can reduce the requirements of the number of GNSS points and the impact of radar decoherence. This provides a new technical approach for studying the law of surface movement in mining subsidence research.

INDEX TERMS DInSAR, genetic algorithm, GNSS, mining subsidence, SBAS.

I. INTRODUCTION

The large-scale development of coal resource production has made an indelible contribution to the development of China's national economy and provided a strong guarantee for the rapid development of China's economy and society. Data from the National Bureau of Statistics show that the total energy consumption in 2020 was 4.97 billion tons of coal, of which 2.82 billion tons was standard coal, and coal consumption accounted for 56.7% of the total domestic energy consumption [1].

The associate editor coordinating the review of this manuscript and approving it for publication was Venkata Ratnam Devanaboyina.

However, the large-scale exploitation of coal resources will inevitably cause a series of ecological environment and social problems. The exploitation of underground coal resources has led to the large-scale subsidence of the surface and destruction of land resources. According to China's coal production and its subsidence rate, the annual land damage caused by the surface collapse of coal mining areas is approximately 33,000 to 47,000 hectares. The annual land damage of coal mining areas is equivalent to the average arable land ownership of 500,000 people in China. By the end of 2004, more than 700,000 hectares of land had collapsed [2], and the number is increasing by 133 hectares every year [3].

Large-scale coal mining collapses have caused the deterioration of the ecological environment in mining areas, and many villages and towns have been destroyed by coal mining subsidence, which poses a direct threat to the social stability of mining areas and has far-reaching impacts on the production and quality of life of the people in such mining areas [4]–[6].

The prediction of subsidence and quantitative calculation of subsidence damage for planned mining operations are effective measures to reduce mining subsidence disasters, and mining subsidence is expected to be an important reference for land reclamation, which has implications for the management of coal mining subsidence, ecological restoration and economic loss reduction in mining areas and is the most important means to reduce the direct and secondary disasters of mining subsidence.

Mining subsidence prediction is expected to be one of the core contents of mining subsidence studies. It is important to the theoretical research and practice of mining subsidence [7].

An accurate prediction model the key to mining subsidence predictions. probabilitical integration method (PIM) is the most widely used model for developing mining subsidence predictions in the mining areas of China [8].

PIM is a mining subsidence prediction method based on stochastic media. The theory was put forward by Polish scholar Litwiniszyn and developed by Baochen Liu [9]. It has been widely used in various mining areas due to its fewer required parameters, simple model processes, and accurate prediction results.

The key point of mining subsidence predictions is obtaining accurate parameters. The empirical research method based on measured data is the best way to obtain PIM parameters. The method to determine the parameters is based on the back analysis of measured mining subsidence deformation data. Then, the mining subsidence deformation can be calculated with these measured parameters with similar geological mining conditions. This is the most reliable way to obtain PIM parameters [10], [11].

The application and popularization of GNSS technology is a great innovation in mining subsidence monitoring efforts. With the development of GPS and the Beidou system, GNSS technology will be increasingly used because of its outstanding advantages, such as all-weather operation, high precision and real-time transmission abilities. Han *et al.* proposed a single-calendar meta-calculation method suitable for mining areas and achieved reliable experimental results based on the analysis of the defects of the existing GPS single-calendar meta-phase settlement method using the unique deformation law of mining subsidence in mining areas [12]. Lin carried out an experimental study on the feasibility of using GPS as the surface deformation monitoring medium for underground mines in his master's thesis, confirmed that its accuracy can meet the requirements of surface deformation analysis, and studied the law of surface and overburden rock deformation combined with numerical simulations [13]. The problems associated with establishing a GPS deformation monitoring network in mining areas, i.e., real-time monitoring requirements, baseline parity issues, deformation analyses and formation characteristics, are discussed in Lua's paper in depth [14]. GPS deformation monitoring technology can reveal the nonlinear characteristics of surface movement. Compared with traditional level measurements, GNSS technology has the following advantages: it requires a simple station set up; there is no need for visibility between adjacent stations; and the three-dimensional displacement information of deformation points can be obtained, thereby reducing workload and monitoring complications. Therefore, GNSS is an all-weather, high-precision, simple operation, automation method that has been widely used in the study of mining subsidence.

However, traditional GNSS data based on point observations to study the law of surface movement have some problems, mainly manifested in the following two aspects:

(1) It is not possible to accurately calculate the subsidence deformation field within the scope of mining impact, and it is difficult to obtain an isomorphic subsidence line or a horizontal moving isographic chart of the subsidence area.

(2) Because of the complexity of the geological, hydrological, geomorphological, and mining conditions of coal seam deposits, the parameters calculated from the discrete point observations are somewhat one-sided.

The application of DInSAR technology makes it possible to monitor surface mining subsidence in low-cost, long-cycle, all-wide basins. InSAR measurement technology is a type of three-dimensional information acquisition technology that was gradually developed in the late 1960s. InSAR technology is widely used to obtain large-scale, high-precision deformation using phase information from differential of two synthetic aperture radar images. Liu *et al.* used time series-based DInSAR technology to monitor the quantitative application of mining subsidence in mining areas and used time series-based DInSAR to extract the forward angle of influence, angle of draw, starting distance and other parameters of different mining stages [15]. A new method of monitoring mining subsidence using a time series synthetic aperture radar image set and studied the average rate of surface subsidence of a mine for many years are studied by Fan *et al.* [16]. The model and algorithm of integrating a multiwavelet platform are proposed in order to solve the three-dimensional deformation field, verify it with the standard measured data, and discuss the sensitivity of the deformation direction [17].

DInSAR technology has become a topic of major interest to mining subsidence research because of its low economic cost and ability to provide 24-hour surface deformation monitoring under all weather conditions at a wide scale. However, it is susceptible to atmospheric interference, and it is difficult to obtain three-dimensional deformation. DInSAR technology is easily decorrelated when the surface movement speed is greater than a certain value. Therefore, it can only be used for short-cycle, small-speed deformation areas, which greatly limits its range of application. Further study is needed for the application of DInSAR technology in the

TABLE 1. Information of Panels 011027 and 01109.

Name	Mining Date	Average Mining Depth (m)	Average Mining Thickness (m)	Dip Angle (°)	Azimuth of strike (°)	Average Mining Velocity (m/day)
011207	2017.08-2019.04	164	1.2	1~3	11	4.3
011809	2017.12-2019.08	188	4	1~3	11	4.5

large-scale engineering application of deformation monitoring in mining areas.

There are several effects can limit its ability to accurately map deformation over mining areas. First, most mining areas are located in nonurban regions in the absence of stable scatterers, which causes decorrelation effects due to temporal changes in scattering characteristics. Second, the fast motion of the active mining area cannot be appropriately reconstructed from the interferometric phase due to aliasing effects. An additional limitation for conventional InSAR techniques is atmospheric artifacts. Ng *et al.* [18] suggested the use of consecutive interferograms with a shorter time gap to detect rapid terrain movements in mining areas. The small baseline subset (SBAS) technique was used in our study.

Based on a small number of GNSS monitoring points, combined with timing series DInSAR technology, this study aimed to obtain accurate, reliable, and fine mining deformation results and use a genetic algorithm model for PIM parameter inversion calculation. The research results can provide a scientific basis to support mining subsidence calculations, construction (or structure) damage assessments, land damage assessments and environmental management efforts.

II. STUDY AREA AND AVAILABLE DATASETS

A. DESCRIPTION OF STUDY AREA

The Jinfeng coal mine belongs to Shenhua Ningxia Coal Industry Group Co., Ltd. It was the first mine established in Majiatan mining area. The mining area is located in Yanchi County, East Ningxia. It is bounded by the Laozhuangzi fault in the north, the Yanzhong Expressway in the south, the Lixinzhuang fault in the west and the Maliu fault in the east of the Majiatan mining area. The mining area is 11.5 $\sim$ 12.0 km long from north to south and 1.9 $\sim$ 3.5 km wide from east to west, covering an area of 41.0 km^2. It mainly mines 3, 4, 6, 12, 17, 18 coal seams, etc., with coal seam dip angles of 5° $\sim$ 60°. The recoverable reserves of the mine are 462.39 Mt, and its service life is 66.1 a. The industrial site and its shafts are on the north side of the Fenghuang transverse fault, with an open and flat terrain, which is also located close to railways and highways. The site average elevation is approximately +1428 m, and the buried depth of the coal seam is 50-300 m. The mine adopts an inclined shaft, an uphill and downhill development system, with 3 shafts of main inclined shaft, an auxiliary inclined shaft, and an air return inclined shaft. The mine is equipped with south and north wing roadway groups, which are divided into five mining areas. The Jinfeng minefield began construction in June 2008, with an annual designed production capacity of 4 million tons/year. In 2014, the Jinfeng coal mine established 6 GNSS real-time dynamic surface movement observation stations in the study area for surface movement monitoring. Due to the high cost of GNSS station construction and maintenance, introducing radar data for surface monitoring has been proposed. The monitoring data of surface mining subsidence are obtained by using ESA Sentinel-1A data. Based on the monitored data combined with GNSS and DInSAR monitoring results, taking the 011809 and 011207 working mining panels as examples, a genetic algorithm combined with PIM is used for mining subsidence predicted parameter inversion. The excavation engineering plan and the ground GNSS point comparison diagram of working panels 011809 and 011207 are shown in Fig. 1.

The basic information of the two working faces is shown in Table 1.

B. INSAR DATA

To extract a high spatial resolution map of ground surface displacement over the mining area, we collected 83 SAR images during the time of 12 Oct 2017-22 Jun 2020 from the Sentinel-1 satellite. The short repeat cycle (12 days) of Sentinel-1 increases our ability to monitor ground displacement with a high gradient in mining areas.

GMTSAR is used to process these SAR images to form differential interferograms [19]. To suppress the geometric and temporal decorrelation effects, we used a temporal threshold of 35 days and a spatial threshold of 150 m to combine the interferograms, and a total of 159 interferograms were constructed (Fig. 2). A 30-m digital elevation model (DEM) from the Shuttle Radar Topography Mission (SRTM) was used to remove the topographical phase component. The interferograms were multi-looked by 8 and 2 in the range and azimuth direction to suppress decorrelated noises, respectively. To ease phase unwrapping, we used a 200-m Gaussian filter to suppress the noise in all the interferograms. The interferograms were then unwrapped by SNAPHU (Statistical-Cost, Network-Flow Algorithm for Phase Unwrapping) software [20].

Finally, the time series of ground displacement at each acquisition points were inverted by the SBAS method as described in Section 3.1.

C. GNSS DATA

The GNSS monitoring points implemented a dynamic real-time monitoring system. The automatic monitoring base station is set in the stable area that is not affected by mining, and the observation station is set above the goaf

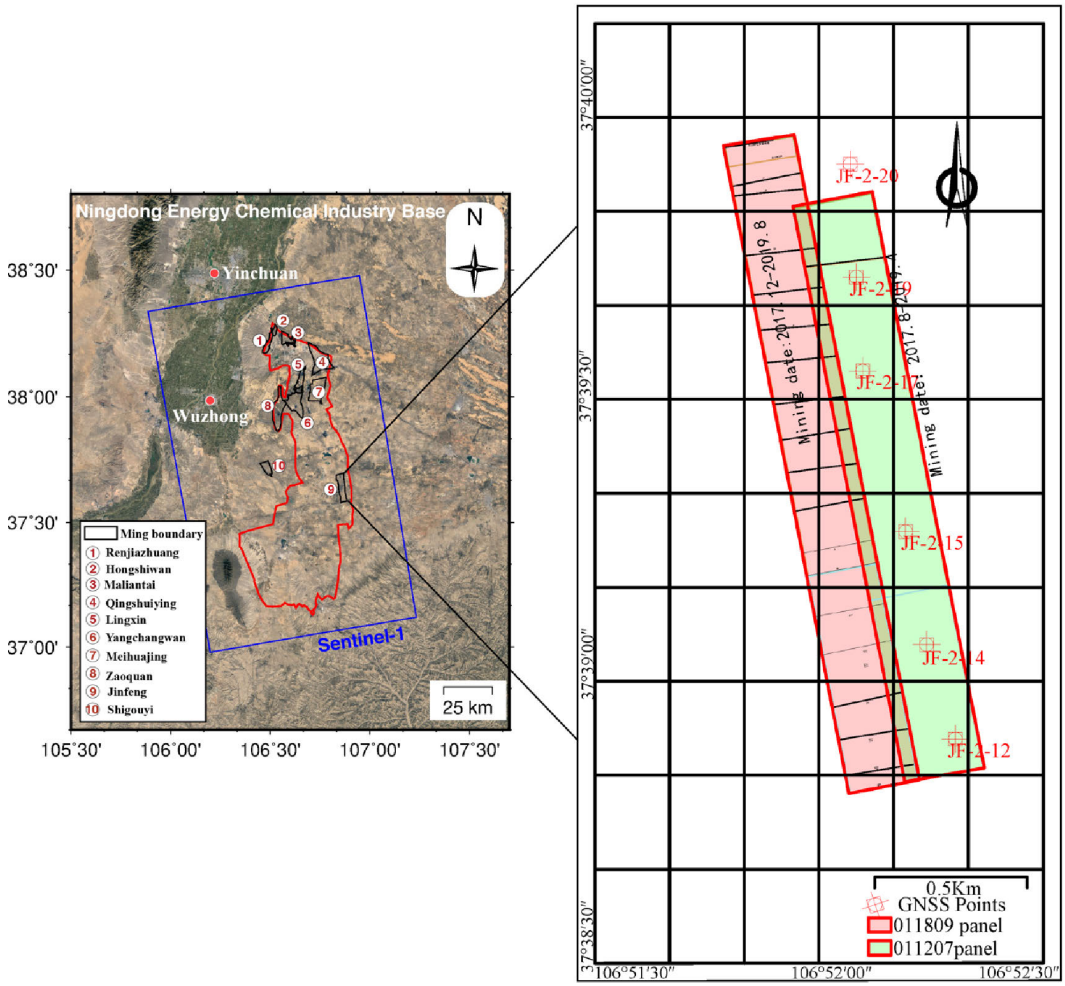

FIGURE 1. Location, the 011809 and 011207 working panels and GNSS points of the Jinfeng coal mine (left image shows the map of the study area. Ten mining areas were located within in the Ningdong Energy Chemical Industry base. We focused on the Jinfeng mine in this study. Right image shows the two working panels in the Jinfeng mine and the corresponding GNSS points).

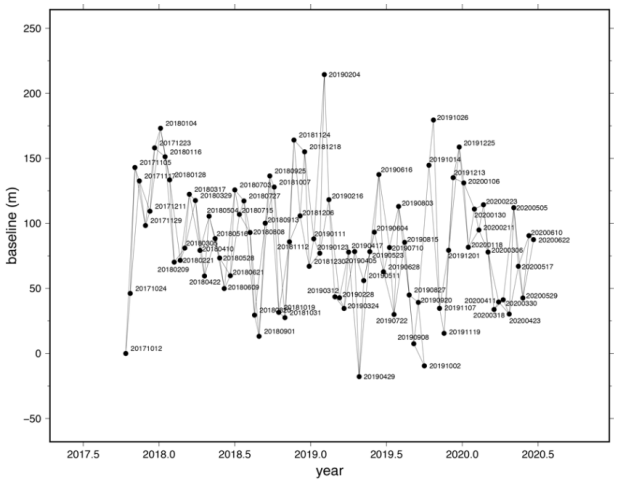

FIGURE 2. Temporal and spatial baseline of small baseline interferograms in this study.

(as shown in Fig. 3). Each automatic observation station and reference point receiver received GPS signals in real time and sent them to the control center through the data communication network, and a fixed time was set to transmit the displacement monitoring data. The GPS data processing software of the control center server calculates the three-dimensional coordinates of each monitoring point by real-time differential analysis. The data analysis software obtains the real-time three-dimensional coordinates of each monitoring point and obtains the variation of the monitoring point by comparison with the initial coordinates. At the same time, the analysis software alarms are established according to the preset warning value. The automatic monitoring and data distributor system is shown in Fig. 4.

III. METHOD

A. SBAS TECHNIQUE

SBAS technique relying on an appropriate combination of interferograms characterized by small spatial and temporal baselines. Due to its short-repeat cycle and regular Sentinel-1 data acquisition, SBAS considerably minimizes decorrelation and topographic error-induced artifacts. The computed small baseline differential interferograms are organized in a linear

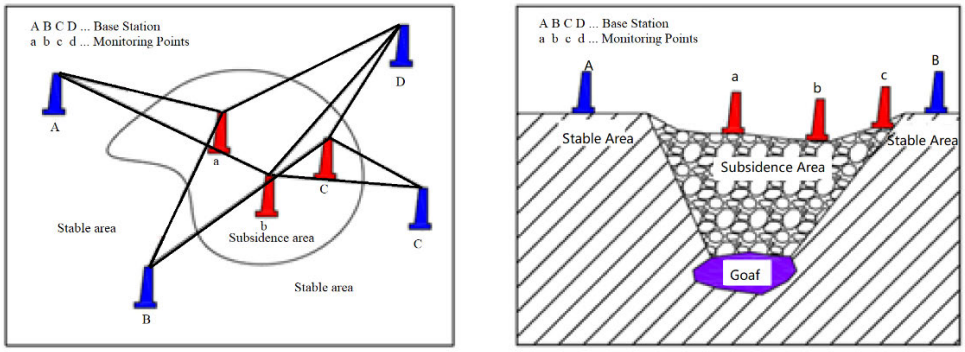

FIGURE 3. Layout of GNSS automatic monitoring points.

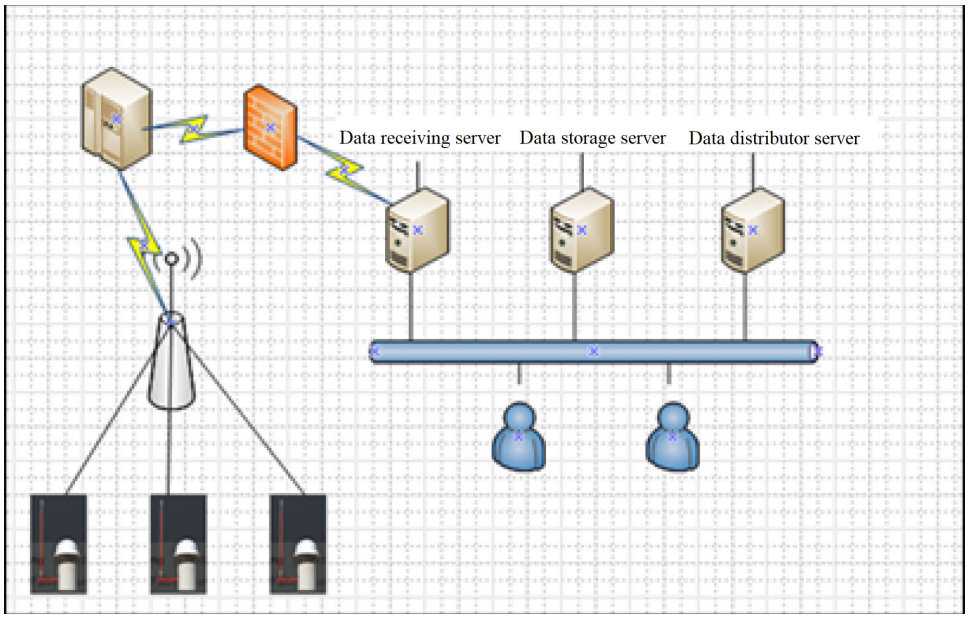

FIGURE 4. Schematic diagram of GNSS automatic monitoring system.

model, as shown in equation (1).

$$B \cdot v = \Delta\phi \tag{1}$$

where B (M by N) is the design matrix defining the interferogram combinations, $\Delta\phi$ is the vector of M known unwrapped phases from M interferograms, and v is the vector of the N unknown phase values associated with the cumulative displacement of N SAR acquisitions in the time series. The solution of time-series phase values associated with ground displacement for each selected coherent pixel is given by equation (2).

$$\hat{v}_N = (B^T B)^{-1} B^T \Delta\phi \tag{2}$$

When all the interferograms are connected and B is full rank, the above least-squares solution can be achieved. However, the matrix B will be ranked as deficient if the small baseline interferograms are separated into different subsets, and the linear system will have infinite solutions [21]. The singular value decomposition (SVD) method is used to "link" the separate small baseline subsets to obtain a minimum-norm least squares (LS) solution, as follows:

$$\hat{v}_N = V \begin{bmatrix} \Sigma^{-1} & 0 \\ 0 & 0 \end{bmatrix} U^T \Delta\phi \tag{3}$$

where V, U and $\Sigma^{-1} = diag(\sigma_1^{-1}, \ldots, \sigma_{N-L+1}^{-1})$ are the SVD decompositions of B, with $N - L + 1$ being the rank of B and L being the number of subsets. In combination with the SBAS inversion, the atmospheric artifacts are filtered out by the common-point stacking method [22]. The resolution of $\hat{v}_N$ is the temporal evolution of the phase, i.e., the displacement time series. The deformation rates are then obtained by fitting the displacement time series to a linear regression.

B. PIM MODEL

The principle of the PIM mining subsidence prediction model is based on random medium theory. According to the basic principle of PIM, the surface subsidence, tilt, curvature, horizontal movement, and horizontal strain of any shape or

multiworking surface can be expressed as a double integral shown in equations (4-8).

$$W(x,y) = \sum_{j=1}^{n} \iint_{D_j} W_0 W_e(x,y) dsdt = \sum_{j=1}^{n} \iint_{D_j} \frac{W_0}{r_j^2} e^{-\pi \frac{(x-s)^2+(y-t)^2}{r_j^2}} dsdt \quad (4)$$

$$i(x,y,\varphi) = \frac{\partial W(x,y)}{\partial x}\cos\varphi + \frac{\partial W(x,y)}{\partial y}\sin\varphi$$

$$K(x,y,\varphi) = \frac{\partial i(x,y,\varphi)}{\partial x}\cos\varphi + \frac{\partial i(x,y,\varphi)}{\partial y}\sin\varphi \quad (5)$$

$$= \sum_{j=1}^{n} \iint_{D_j} \left[\frac{-2\pi W_0}{r_j^4} \{1 - \frac{2\pi}{r_j^2}[(x-s)\cos\varphi + (y-t)\sin\varphi]^2\} e^{-\pi \frac{(x-s)^2+(y-t)^2}{r_j^2}} \right] dsdt \quad (6)$$

$$U(x,y,\varphi) = \sum_{j=1}^{n} \iint_{D_j} \frac{-2\pi b W_0}{r_j^3} \{[(x-s)\cos\varphi + (y-t)\sin\varphi] e^{-\pi \frac{(x-s)^2+(y-t)^2}{r_j^2}} \} \quad (7)$$

$$\varepsilon(x,y,\varphi) = \sum_{j=1}^{n} \iint_{D_j} \left[\frac{-2\pi b W_0}{r_j^3} \{1 - \frac{2\pi}{r_j^2}[(x-s)\cos\varphi + (y-t)\sin\varphi]^2\} e^{-\pi \frac{(x-s)^2+(y-t)^2}{r_j^2}} \right] dsdt \quad (8)$$

where W_0 is the maximum subsidence of critical mining or supercritical mining, and $W_0 = mq\cos\alpha$. Other parameters are defined as follows:

r—major influence radius, $r = H/tan\beta$
H—mining depth; q—subsidence factor
b—horizontal movement factor
m—mine thickness
$tan\beta$—tangent of major influence angle
D— mining area
n—number of mining panels
α—dip angle of coal seam.

A MATLAB program based on PIM that can predict the mining subsidence of any shape multi-working panels was developed. It provides a calculation interface for parameter inversion with the genetic algorithm.

C. PARAMETER INVERSION MODEL BASED ON MULTISOURCE MONITORING DATA

When using multisource monitoring data for PIM inversion, the coupling and selection model of monitoring results, such as DInSAR and GNSS, must be established, and the results of the surface vector movement must be obtained. Surface movement fitting was used in the PIM inversion model. First, a simulation of the three-dimensional surface movement was obtained from PIM, and inversion calculation was carried out on the basis of the minimum square of error between PIM and field measured data. The calculation results were output if the inverse result met the requirements; otherwise, the calculation continued using the obtained parameters as the initial values. The flow chart is shown in Fig. 5.

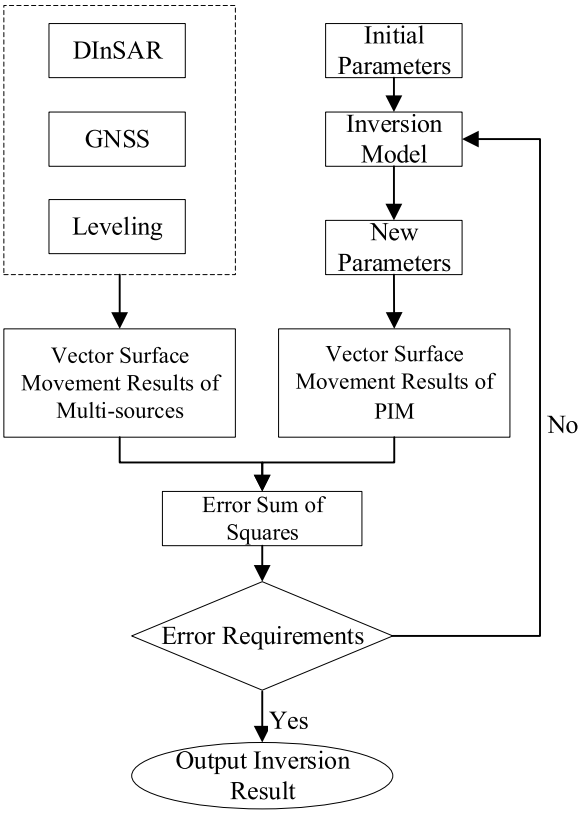

FIGURE 5. Flow chart of PIM parameter inversion based on multisource monitoring results.

1) CALCULATION AND SELECTION OF INITIAL PARAMETERS

The initial subsidence factor can be calculated by equation (9).

$$q = \frac{W_0}{m\cos\alpha} \quad (9)$$

where q is the subsidence factor; W_0 is the maximum subsidence of critical mining or supercritical mining, $W_0 = mq\cos\alpha$; m is the mining thickness (mm); and α is the dip angle of the coal seam (°).

Other initial parameter values can be selected based on experience. For example, $tan\beta$ can be 1.6∼2.2, and the horizontal movement factor b is initially set to 0.3.

2) OPTIMIZATION INVERSION WITH GENETIC ALGORITHM

At present, there are many algorithms available for PIM inversion, such as direct search algorithms and pattern search algorithms. Additionally, some are based on bionic group intelligent algorithms, such as particle groups, ant colonies, bee colonies, etc. In this study, a genetic algorithm was selected as the basic algorithm for calculation. Although it is

a bionic global search optimization algorithm belonging to the same group algorithm as particle swarm optimization (PSO), the GA can solve the discrete problem, has a mature convergence analysis method and can estimate the convergence speed.

Genetic algorithms start with a population that represents a potential solution to the problem, while a population consists of a certain number of individuals encoded by genes. Each individual is actually a chromosome-characterized entity. Chromosomes act as the main carriers of genetic material; essentially, they are a collection of multiple genes. Then, it is necessary to encode a mapped phenotype to a give genotype. Binary encoding and real value encoding are the most commonly used encoding methods. After the first generation of populations is produced, according to the principle of survival of the fittest (function), generation-by-generation evolution produces an increasingly good approximate solution. In each generation, the individual is selected according to the value of the individual's fitness in the problem domain. A new generation solution set can be produced with the help of natural genetic operators combined with crossover and mutation. This process will result in a population that is more environmentally adaptable to the natural evolution of later generations than the previous generation, and the optimal individuals in the last population are decoded as an approximate optimal solution to the problem. The flow chart of GA is shown in Fig. 6.

Genetic algorithms have been widely used in production scheduling, automatic control, image processing and machine learning application because of their advantages of parallelism, stability, randomness, and extendibility.

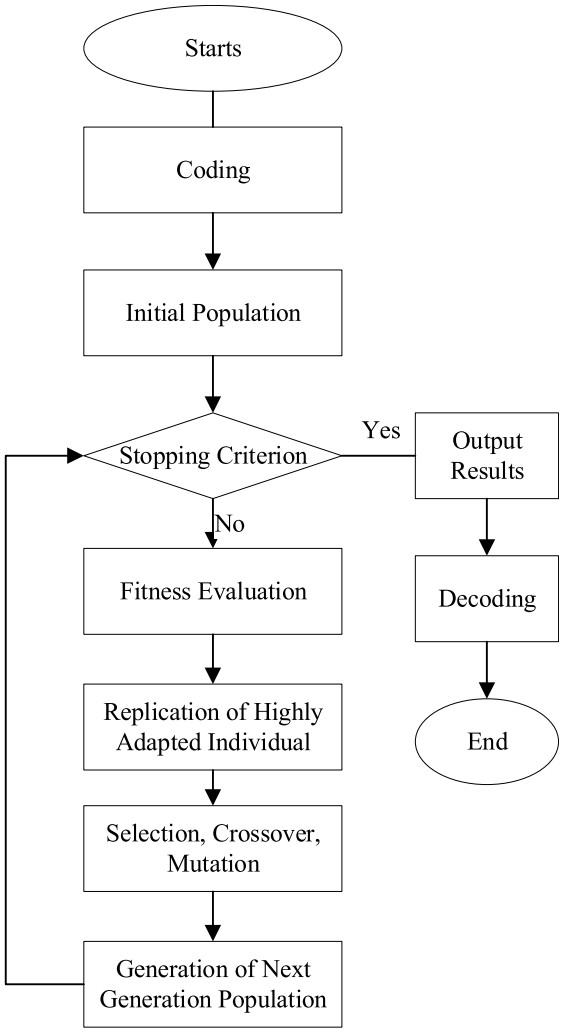

FIGURE 6. Flowchart of genetic algorithm.

3) SUM OF SQUARED ERROR AND FITNESS FUNCTION

The deformation results of DInSAR monitoring occurs along the radar line of sight; the result of GNSS monitoring is the three-dimensional deformation, which can be decomposed into north-south, east-west and subsidence according to the resulting coordinates; the result of leveling monitoring is displacement in the plumb direction. Therefore, the difference between the results calculated by PIM under certain parameters and measured is selected as the basis of the fitness function for the genetic algorithm. The probability integral values stimulated by the DInSAR LOS deformation and GNSS three-dimensional deformation methods can be calculated by (9-10). The settlement value obtained from leveling monitoring can be directly compared with the subsidence results of PIM.

The results of the DInSAR LOS deformation simulated by PIM can be calculated according to equation (10).

$$W_{LOS} = W\cos\theta - \sin\theta \times \left[U_N \cos\left(\alpha - \frac{3\pi}{2}\right) + U_E \sin\left(\alpha - \frac{3\pi}{2}\right)\right] \quad (10)$$

where W_{LOS} is the result simulated by PIM (mm); W is the result calculated by PIM(mm); θ is radar incidence angle(°); U_N is horizontal movement along the north-south direction (mm); U_E is horizontal movement along the north-south direction (mm); and α is the azimuth of the radar orbit.

The results of GNSS deformation simulated by PIM can be calculated according to equation (11)

$$W_{GNSS} = \sqrt{W^2 + U_N^2 + U_E^2} \quad (11)$$

4) CALCULATION OF THE SSE

The inversion method is based on the SSE between the measured and simulated deformation values. The calculation method of the SSE is shown in equation (12).

$$[VV] = \sum_{i=1}^{n} (S - W)^2 \quad (12)$$

where $[VV]$ is the SSE between the measured and simulated deformation values; S is the measured LOS surface movement DInSAR and the 3D movement for GNSS and subsidence for leveling; and W is the surface movement calculated by PIM.

TABLE 2. The Subsidence and Displacement of GNSS Points Over Panels 011207 and 011809.

Points ID	Distance (m)	Subsidence (mm)	Displacement along the north-south direction (mm)	Displacement along the west-east (mm)
JF-2-12	453	1244	-32	4
JF-2-14	776	1254	-214	-34
JF-2-15	1153	1373	-273	-12
JF-2-17	1697	1398	-594	-57
JF-2-19	2003	1251	-225	-43
JF-2-20	2369	52	-42	-16

Note: The north-south displacement is positive to the north, and the east-west displacement is positive to the east.

TABLE 3. The Inversion PIM Parameters of the Jinfeng coal Mine.

q	b	$tan\beta$	θ^0	S
0.87	0.3	1.8	84	0.05 H

The fitness function of the genetic algorithm is calculated by the reciprocal of the sum of squares of the errors. The larger the fitness function is, the better the inversion result will be.

IV. RESULTS AND ANALYSIS

A. GNSS DEFORMATION RESULTS

To analyze the final surface movement caused by mining and reduce the influence of the surrounding goaf on the surface subsidence monitoring results, the final monitoring results of Jf-2-12, Jf-2-14, Jf-2-15, Jf-2-17, Jf-2-19 and Jf-2-20 (as shown in Table 2) are taken as the basis for the final parameter inversion.

B. INSAR DEFORMATION RESULTS

The ground deformation map covering the Jinfeng mining area derived from SBAS InSAR is shown in Fig. 7. The data acquisition is regular and uniform in time, which improves the performance of fast deformation extraction. The time range of the Sentinel-1 data used in this monitoring project is from October 12, 2017, to June 22, 2020, with a total of 83 periods of track No. 157 data. SBAS InSAR technology is used to calculate the surface movement and deformation. The results of the ground subsidence time series of DInSAR points are shown in Fig. 8.

The SBAS calculation results of working panels 011207 and 011809 in the Jinfeng coal mine are shown in Fig. 8. In the SBAS results, reliable points are extracted according to the coherence coefficient. Points with coherence coefficients less than 0.2 are filtered. The filtered units are selected as the basis of parameter inversion.

C. PARAMETERS INVERSION RESULTS

Based on the comprehensive utilization of GNSS monitoring results and SBAS settlement monitoring results, the parameters used in the probability integral method of surface movement obtained by inversion are shown in Table 3.

We use the PIM parameters displayed in Table 3 to calculate the subsidence and horizontal displacement of panels 011207 and 011809. The comparison results are shown in Fig. 9.

D. ANALYSIS

The comparison of SBAS results with GNSS deformation showed that the SBAS underestimated deformations, indicating that the rapid deformation rates (exceeding 30 mm/day) in this mining panel exceed the capabilities of the SBAS method. Ambiguity in the unwrapping results in the limitation of the maximum differential deformation rate between two neighbouring pixels that can be measured by InSAR. This value is limited to $\lambda/4$ over the revisiting time between two consecutive SAR acquisitions, where λ is the wavelength of the radar signal. The constellation of Sentinel-1A and 1B satellites, forms a revisit period of six days for the C-band sensors with a wavelength of 5.6 cm, which leads to a theoretical maximum deformation rate of 85 cm/year detectable by multi-temporal InSAR method [23]. In addition, the maximum detectable rate of the subsidence trough is also dependent on the spatial resolution of the radar image. To avoid decorrelated effects from SBAS results, we selected deformation from pixels with coherence larger than 0.8 in PIM parameter inversion. Deformations at pixels with high coherence together with the six GNSS stations were used for the input data in the PIM parameters inversion.

The PIM parameters inversed based on DInSAR and GNSS was used same parameters for two panels 011207 and 011809, the reasons were listed as follow:

(1) The 011207 and 011809's excavation time were 4 months apart. The geological conditions of this area determine that the subsidence speed is fast after mining, and the subsidence active period and decline period are truly short. It is enough for the first layer to full subsidence in 4 months.

(2) Both coal seam of 011207 and 011809 are horizontal coal seams. The parameters of those two seams have only small different.

(3) The mine depth of both panels is small. And the interval between two coal seams is 24m. The repeat mining influence is small.

(4) If repeated mining considered, a parameter will be added, which makes the problem more complicated and the result less reliable.

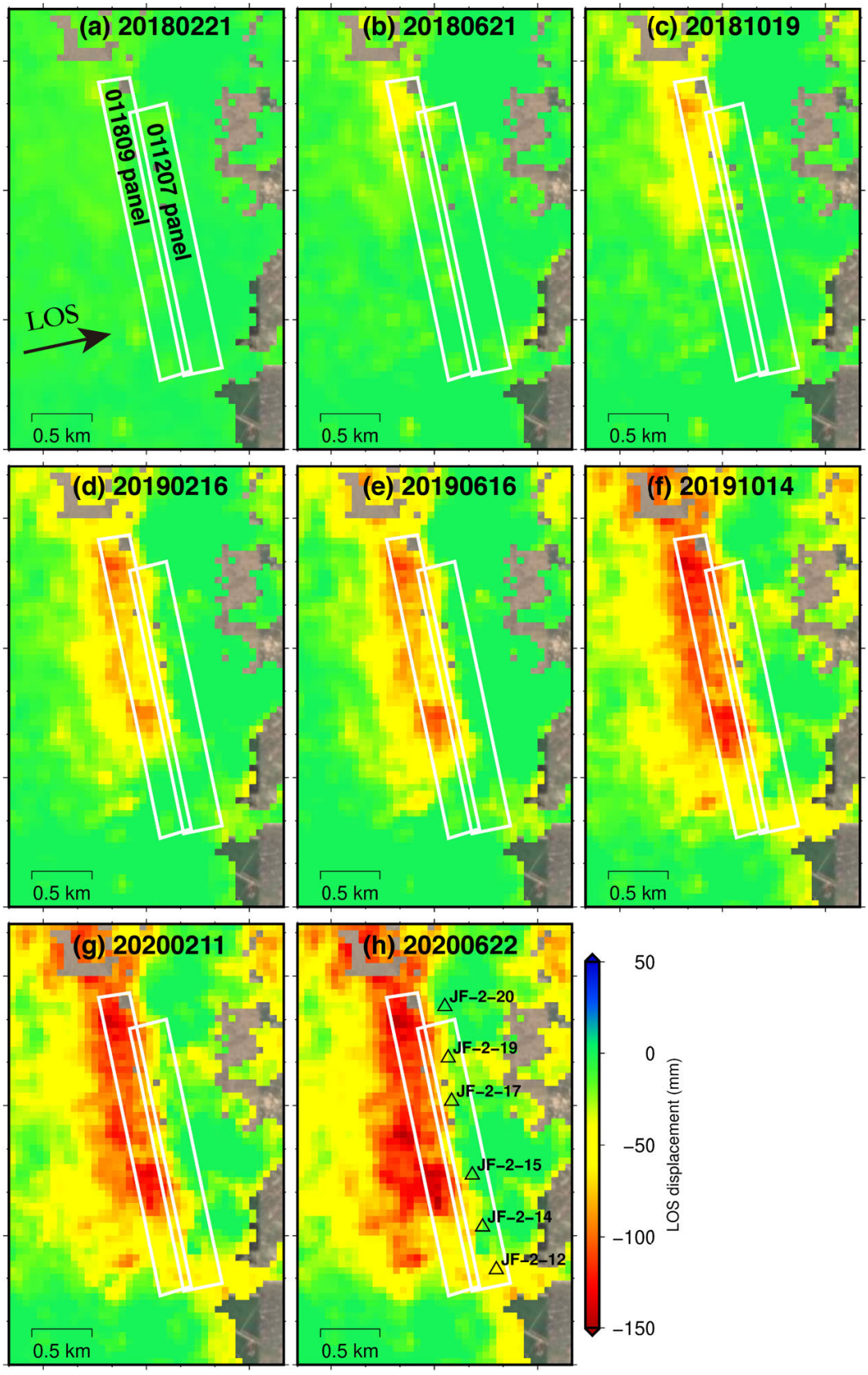

FIGURE 7. Every 4 months of advancement of deformation maps in Jinfeng mine obtained from the SBAS InSAR technique. The triangles in (h) indicate the locations of the GPS stations.

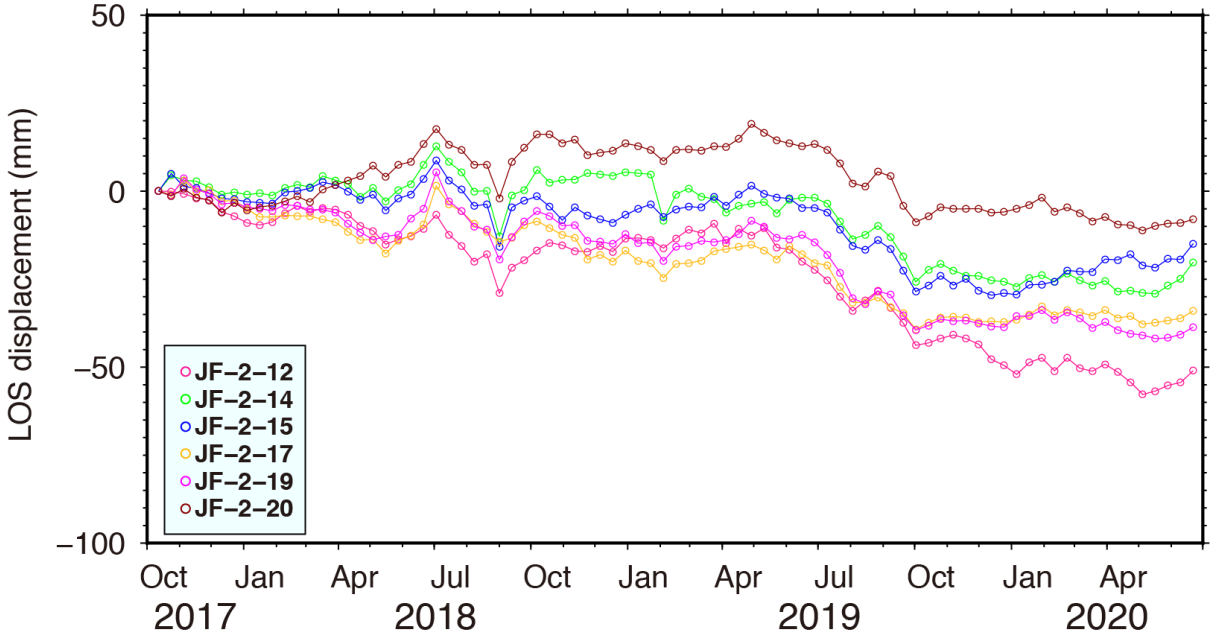

FIGURE 8. InSAR time series deformation at 6 GNSS monitoring points in the Jinfeng coal mine (October 12, 2017 - June 22, 2020).

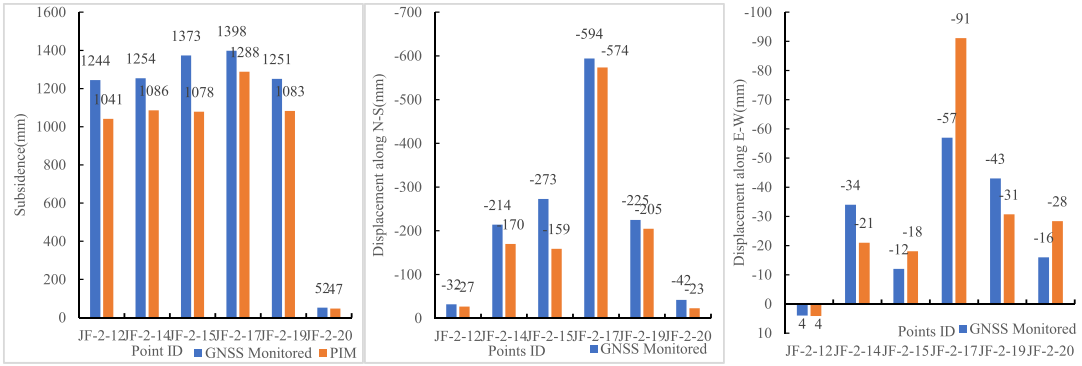

FIGURE 9. Fitting effect of inversion subsidence results and measured results.

V. DISCUSSION

Fig. 9 show that the measured surface movement results are consistent with the inversion results. Using genetic algorithm inversion for surface PIM parameter can effectively reduce the fitness function to a local minimum. The predicted parameters obtained by inversion are used to calculate the mining subsidence prediction, and the calculated results are consistent with the actual surface movement results, which shows that the genetic algorithm is useful for calculating the parameters needed by the multi-working face probability integration method. A genetic algorithm can be used to retrieve the parameters used by the PIM of surface movement under the influence of multiple mining faces. Compared with the direct search algorithm, this method has a higher accuracy and a higher efficiency. The accuracy of the direct search algorithm is related to the selection of the initial value, and it easily falls into the trap of a local minimum. Compared with the least squares' method, the genetic algorithm can optimize the PIM parameters of multiple working panels, which is difficult to achieve when employing the least squares method. In addition, due to the correlation between the parameters, the least square method is more sensitive to the selection of the initial value, and an inappropriate initial value can easily lead to the least square equation not being inversed; thus, the parameters of the probability integral method cannot be solved. The genetic algorithm can prevent optimization from falling into a local minimum through a mutation mechanism, which can effectively realize the global optimization of multiple parameters. It is a multiparameter optimization method with a high accuracy and efficiency. The experimental results show that this method is superior to the traditional direct search algorithm in terms of its calculation accuracy and efficiency, and it can be used for the back analysis calculation of the surface movement-based PIM parameters of multiple mining faces, and the obtained surface movement PIM parameters are reliable.

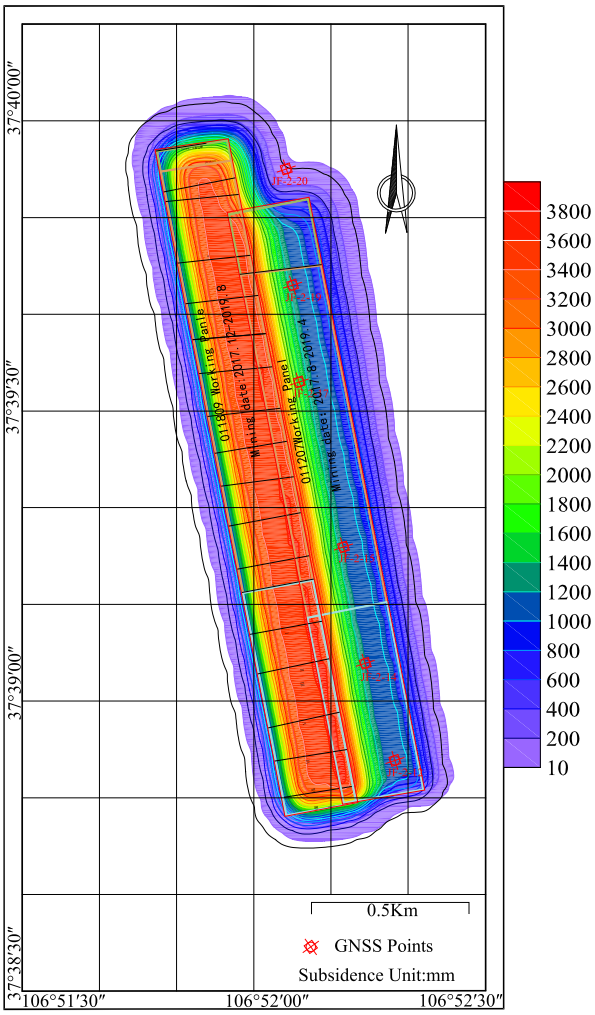

FIGURE 10. Mining subsidence prediction results of the 011207 and 011809 working panels.

The parameters of the probability integral method obtained by inversion are used to predict the subsidence of working faces 011207 and 011809. The calculation results are shown in Fig. 10.

VI. CONCLUSION

(1) According to the LOS deformation obtained by SBAS-DInSAR and the three-dimensional deformation obtained by GNSS, a genetic algorithm parameter inversion model was proposed using three-dimensional surface movement. The three-dimensional deformation includes the three-dimensional vector sum of the subsidence and horizontal movement of any point on the surface, which is the real amount of surface movement. It can avoid the phenomenon of traditional methods that consider subsidence and horizontal movement separately. Three-dimensional surface movement provides full multisource monitoring information for PIM parameter inversion, which can improve the reliability of the inversion results.

(2) Combined with 6 GNSS online monitoring locations and 83 Sentinel-1A radar data points, the surface movement and deformation values of the 011207 and 011809 working faces in the Jinfeng coal mine of Ningxia were obtained. Due to a lack of GNSS monitoring points and the large distance between those points, it is difficult to guarantee the accuracy of the results using only GNSS points to perform the PIM inversion. SBAS-DInSAR monitoring results can effectively address the problem of insufficient monitoring data. The application of D-InSAR can reduce the cost of traditional monitoring methods and improve the efficiency of monitoring. It is a simple and effective method that can be implemented to improve the accuracy of PIM parameter inversion.

(3) According to DInSAR LOS monitoring results and GNSS three-dimensional deformation monitoring results, using the constructed three-dimensional deformation genetic inversion model, Jinfeng coal mine surface movement PIM parameters were obtained, with a subsidence coefficient of 0.87, a horizontal movement coefficient of 0.3, a main influence angle tangent of 1.8, a mining influence propagation angle of 84° and a point-derived inflection offset of 0.05 H. The calculated results are in good agreement with the measured results, which indicates that it is feasible to couple the GNSS and SBAS-DInSAR monitoring results for PIM parameter inversion. The research results can provide a basic basis for subsidence law research and damage prevention in mining.

ACKNOWLEDGMENT

The authors would like to thank the AJE's professional grammar, spelling, and editing services. All the Sentinel data were freely downloaded from ESA, without which this publication would not have been possible.

REFERENCES

[1] National Bureau of Statistics of the People's Republic of China. *National Bureau of Statistics of the People' Republic of China*. Government. National Bureau of Statistics. Accessed: Feb. 28, 2020. [Online]. Available: http://www.stats.gov.cn/tjsj/zxfb/202002/t20200228_1728913.html

[2] L. Li, "Mine collapse and economic transformation in the cities with coal mines," *Jinyang Academic J.*, vol. 5, pp. 56–60, May 2006.

[3] W. Zhang, Y. Gong, X. Luo, L. Hu, S. Zhang, and X. Deng, "Research on the development of coal mining subsidence land under the demand of sustainable development," in *Proc. 6th Na. Graduate Academic Conf. Geography*, Ürümqi, China, Jun. 2011, pp. 21–22.

[4] J. Li, B. Gao, and Z. Wu, "Analysis of surface movement characteristic observation under the condition of extremely incompletely mining in deep mine," *Coal Mining Technol.*, vol. 12, no. 6, pp. 60–63, Jun. 2007.

[5] Z. Tan and K. Deng, *Theory and Practice of Coal Mining Under Buildings*. Xuzhou, China: China Univ. Mining and Technology Press, 2007.

[6] P. Li and Z. Tan, *Surface Subsidence Law of Deep Mining, and its Application*. Beijing, China: Surveying and Mapping Press, 2018.

[7] Y. Zou, K. Deng, and W. Ma, *Mining Subsidence Engineering*. Xuzhou, China: China Univ. Mining and Technology Press, 2003.

[8] B. Hu, H. Zhang, and B. Shen, *Guidelines for Coal Pillar Setting and Coal Mining Under Buildings, Water Bodies, Railways and Main Roadways*. Beijing, China: China Coal Industry Publishing House, 2017.

[9] J. Litwiniszyn, "Stochastic methods in mechanics of granular bodies," in *Stochastic Methods in Mechanics of Granular Bodies: Course held at the Department of General Mechanics*, J. Litwiniszyn, Ed. Vienna, Austria: Springer, Oct. 1974, pp. 5–9.

[10] Y. Li and W. Liu, "Present situation and prospect of methods on predicting mining subsidence," *Sichuan Surveying Mapping*, vol. 21, no. 3, pp. 99–102, Mar. 1998.

[11] Z. Yi, Q. Zhang, and S. Han, "Prediction approaches about subsidence of rock layer and ground surface in a mine," *Exp. Inf. Mining Ind.*, vol. 7, pp. 17–21, Jul. 2007.
[12] B. Han, J. Ou, S. Cheng, and G. Liu, "A new GPS single epoch phase processing algorithm and its application in mining subsidence surveying," *J. China Coal Soc.*, vol. 27, no. 5, pp. 479–482, Apr. 2002.
[13] J. Lin, "Surface deformation analysis and forecast study of the underground mining mine based on GPS monitoring," M.S. thesis, Inst. Rock Soil Mech. Chin. Academy Sci., Wuhan, China, 2009.
[14] Y. Luan and L. Han, "GPS monitoring technology and analysis on mine deformation," *Eng. Surveying Mapping*, vol. 2, pp. 49–51, Feb. 2002.
[15] Z. Liu, Z. Bian, F. Lv, and B. Dong, "Subsidence monitoring caused by repeated excavation with time-series DInSAR," *J. Mining Saf. Eng.*, vol. 30, no. 3, pp. 390–395, Mar. 2013.
[16] H. Fan, K. Deng, J. Xue, and C. Zhu, "An experimental research on using time series SAR images to monitor mining subsidence," *Saf. Coal Mines*, vol. 42, no. 2, pp. 15–18, Feb. 2011.
[17] C. Zhu, K. Deng, J. Zhang, Y. Zhang, H. Fan, and L. Zhang, "Three-dimensional deformation field detection based on multi-source SAR imagery in mining area," *J. China Coal Soc.*, vol. 39, no. 4, pp. 673–678, Apr. 2014.
[18] A. H.-M. Ng, L. Ge, Y. Yan, X. Li, H.-C. Chang, K. Zhang, and C. Rizos, "Mapping accumulated mine subsidence using small stack of SAR differential interferograms in the Southern coalfield of new South Wales, Australia," *Eng. Geol.*, vol. 115, nos. 1–2, pp. 1–15, Sep. 2010, doi: 10.1016/j.enggeo.2010.07.004.
[19] X. Xu, D. T. Sandwell, E. Tymofyeyeva, A. Gonzalez-Ortega, and X. Tong, "Tectonic and anthropogenic deformation at the Cerro Prieto geothermal step-over revealed by sentinel-1A InSAR," *IEEE Trans. Geosci. Remote Sens.*, vol. 55, no. 9, pp. 5284–5292, Sep. 2017, doi: 10.1109/TGRS.2017.2704593.
[20] C. W. Chen and H. A. Zebker, "Two-dimensional phase unwrapping with use of statistical models for cost functions in nonlinear optimization," *J. Opt. Soc. Amer. A, Opt. Image Sci.*, vol. 18, no. 2, pp. 338–351, 2001, doi: 10.1364/josaa.18.000338.
[21] P. Berardino, G. Fornaro, R. Lanari, and E. Sansosti, "A new algorithm for surface deformation monitoring based on small baseline differential SAR interferograms," *IEEE Trans. Geosci. Remote Sens.*, vol. 40, no. 11, pp. 2375–2383, Nov. 2002, doi: 10.1109/TGRS.2002.803792.
[22] A. Pepe and F. Calò, "A review of interferometric synthetic aperture RADAR (InSAR) multi-track approaches for the retrieval of Earth's surface displacements," *Appl. Sci.*, vol. 7, no. 12, p. 1264, Dec. 2017, doi: 10.3390/app7121264.
[23] M. Ilieva, P. Polanin, A. Borkowski, P. Gruchlik, K. Smolak, A. Kowalski, and W. Rohm, "Mining deformation life cycle in the light of InSAR and deformation models," *Remote Sens.*, vol. 11, no. 7, p. 745, Mar. 2019, doi: 10.3390/rs11070745.

GUORUI WANG received the master's degree in geological engineering from the China University of Mining and Technology (Beijing), China, in 2016, where he is currently pursuing the Ph.D. degree. His current research interests include mine environmental protection, underground water, and prevention of geological hazard.

QIANG WU received the Ph.D. degree in hydrogeology from the China University of Geosciences (Beijing), in 1991. He is currently an Academician with the Chinese Academy of Engineering, a Professor with the China University of mining and Technology (Beijing), China, the Director of the National Research Center for coal mine water disaster prevention and control engineering technology, the Vice Chairman of the International Mine Water Association (IMWA), the Chairman of the China National Committee of International Mine Water Association (IMWA), the Leader of Hydrogeology expert group of the State Coal Mine Safety Supervision Bureau Deputy Editor-in-Chief of environment, a member of the National Committee of China Association of Science and Technology and the Technical Committee of State Administration of Work Safety, and the Executive Director of the China Coal Society and the China Geological Society. His current research interests include teaching and scientific research of mine water control and resource utilization.

PEIXIAN LI received the Ph.D. degree in geodesy and surveying engineering from the China University of Mining and Technology (Beijing), Xuzhou, China, in 2012. He is currently an Associate Professor of geodesy and surveying with the Geomatics and Land Use Department, China University of Mining and Technology (Beijing).

XIMIN CUI received the Ph.D. degree in mine engineering mechanics from the China University of Mining and Technology (Beijing), Xuzhou, China, in 1996. He is currently a Professor of geodesy and surveying with the geomatics and land use department, China University of Mining and Technology (Beijing). His current research interests include deformation monitor and rock mechanics.

YONGFENG GONG received the master's degree in environmental engineering from Chang' An University, Xian, China, in 2010. He is currently pursuing the Ph.D. degree with the China University of Geosciences. His current research interests include underground water and prevention of geological hazard.

JIA ZHANG received the master's degree in hydrology and water resources from Chang' An University, China, in 2016. Her current research interests include underground water and geological disaster monitoring.

WEI TANG received the Ph.D. degree from the State Key Laboratory of Information Engineering in Surveying, Mapping and Remote Sensing, Wuhan University, Wuhan, China, in 2017. He is currently a Lecturer in monitoring and modeling of ground surface deformations related to mining activities, groundwater extraction, oil exploitation, and CO_2 injection.